

Linear-response formula for finite-frequency thermal conductance of open systemsAbhishek Dhar,¹ Onuttom Narayan,² Anupam Kundu,¹ and Keiji Saito³¹*Raman Research Institute, Bangalore 560080, India*²*Department of Physics, University of California, Santa Cruz, California 95064, USA*³*Department of Physics, Graduate School of Science, University of Tokyo, Tokyo 113-0033, Japan*

(Received 27 August 2010; published 3 January 2011)

An exact linear-response expression is obtained for the heat current in a classical Hamiltonian system coupled to heat baths with time-dependent temperatures. The expression is equally valid at zero and finite frequencies. We present numerical results on the frequency dependence of the response function for three different one-dimensional models of coupled oscillators connected to Langevin baths with oscillating temperatures. For momentum conserving systems, a low-frequency peak is seen that is higher than the zero-frequency response for large systems. For momentum nonconserving systems, there is no low-frequency peak. The momentum nonconserving system is expected to satisfy Fourier's law; however, at the single bond level, we do not see any clear agreement with the predictions of the diffusion equation even at low frequencies. We also derive an exact analytical expression for the response of a chain of harmonic oscillators to a (not necessarily small) temperature difference; the agreement with the linear-response simulation results for the same system is excellent.

DOI: [10.1103/PhysRevE.83.011101](https://doi.org/10.1103/PhysRevE.83.011101)

PACS number(s): 05.60.Cd, 05.70.Ln

I. INTRODUCTION

In many low-dimensional systems, heat transport unexpectedly violates Fourier's law of heat conduction [1–3]. This can be because of integrability or proximity to integrability, which is more common in low dimensions, as recognized starting from the Fermi-Pasta-Ulam (FPU) model [4]. Alternatively, even ergodic low-dimensional systems can show anomalous heat conduction, with the conductivity diverging with system size, if they conserve momentum. Apart from the theoretical interest, understanding heat transport in such systems is of relevance to heat conduction in carbon nanotubes [5].

Most of the recent activity [2,3] in this field has dealt with the zero-frequency conductivity. But time-dependent temperature sources have been discussed in experimental situations in the context of measuring the frequency-dependent thermal conductivity [6,7] and specific heat [8] of glassy systems. Theoretically, there have been a few studies on the frequency-dependent thermal current response using a microscopic approach, based on Luttinger's derivation of the Green-Kubo formula and a hypothesis about the equality of certain transport coefficients [9], and using a phenomenological approach [10]. A recent paper studied thermal ratchet effects in an inhomogeneous anharmonic chain coupled to baths with time-dependent temperatures [11,12].

In this paper, we adopt a different approach: we find the linear heat conductance of a system placed in contact with two heat reservoirs with time-dependent temperatures, $T_L(t)$ and $T_R(t)$, respectively. Physically the notion of bath temperatures oscillating in time make sense if we assume that the frequency of oscillation is much smaller compared to time scales for local thermal equilibration in the reservoirs. An exact expression (in the linear-response regime) for the heat current due to a small oscillating temperature difference between the reservoirs is obtained.

Our earlier result [13] obtained the zero-frequency conductance of a finite system rather than the conductivity in the infinite system limit. Thus the thermodynamic limit was not taken first (in fact, not at all), in contrast to the standard

Green-Kubo formula [14], which cannot be applied when the infinite system conductivity diverges. Our expression for the zero-frequency conductance involved the heat current autocorrelation function for an open system. The extension to finite frequencies in this paper follows the same approach, with the response now depending on the position inside the system where the current is measured.

We also show results of numerical simulations for the frequency-dependent response function by measuring the appropriate correlation function. For one-dimensional momentum conserving anharmonic crystals, we find a resonant response at a frequency of $\omega \sim 1/N$ for a chain of N particles due to sound waves propagating from one end of the system to the other. As N increases, the resonance gets broader and its height decreases slightly. However, its height relative to the zero-frequency response *increases*, and for large N this resonance is stronger than the zero-frequency response.

We find that the low-frequency peak disappears for systems where momentum is not conserved. Fourier's law is known to be valid for such systems, so that the heat current should satisfy the diffusion equation. If one compares the numerical results for the frequency-dependent heat current with the prediction from the diffusion equation at the single bond level, there seem to be substantial discrepancies. This suggests that the hydrodynamic limit is somewhat subtle and may require study of larger system sizes with appropriate spatial and temporal coarse graining.

Numerical simulations for the frequency-dependent response function of a one-dimensional harmonic crystal, and an exact analytical expression for the full response (for finite ΔT) of the same, are also presented. For a harmonic system the full response is also linear and hence we expect the linear-response result to agree with the exact-response function. Indeed we find excellent agreement between the numerical simulations of the expression of the linear-response and the numerically evaluated exact-response expression.

All three systems mentioned previously also show a high-frequency peak in the response function, whose location is independent of N . One can loosely ascribe this to the fact that

the dynamics in the interior of the system are underdamped (actually, undamped), so that particles approaching each other recoil, and the heat current autocorrelation function shows rapid oscillations in the temporal domain. Such high-frequency oscillations are not seen in hard particle models, such as the Random Collision Model [15]. This is discussed further when we derive the analytical expression for the harmonic oscillator. However, a quantitative understanding of the high-frequency peak is lacking.

II. OSCILLATOR CHAINS WITH LANGEVIN BATHS

We follow the derivation of Ref. [13] to obtain the finite-frequency heat conductance of an oscillator chain with Langevin baths at the ends; more detail is provided in Ref. [13]. Consider the motion of N particles on a one-dimensional lattice, described by the following Hamiltonian:

$$H = \frac{1}{2} \sum_{l=1}^N m_l v_l^2 + \sum_{l=1}^N U(x_l - x_{l+1}) + \sum_{l=1}^N V(x_l), \quad (1)$$

where $\mathbf{x} = \{x_l\}$ and $\mathbf{v} = \{v_l\}$, with $l = 1, 2, \dots, N$, are the displacements of the particles about their equilibrium positions and their velocities and $\{m_l\}$ are their masses. We assume fixed boundary conditions, $x_0 = x_{N+1} = 0$. The particles 1 and N are connected to white noise Langevin heat baths at time-varying temperatures $T_L(t)$ and $T_R(t)$. Thus the equations of motion are

$$m_l \dot{v}_l = -\frac{\partial}{\partial x_l} [U(x_{l-1} - x_l) + U(x_l - x_{l+1}) + V(x_l)] + \delta_{l,1} [\eta_L(t) - \gamma_L v_1] + \delta_{l,N} [\eta_R(t) - \gamma_R v_N], \quad (2)$$

for $l = 1, 2, \dots, N$. Here $\eta_{L,R}(t)$ are uncorrelated zero mean Gaussian noise terms satisfying the fluctuation dissipation relations

$$\langle \eta_{L,R}(t) \eta_{L,R}(t') \rangle_\eta = 2\gamma_{L,R} k_B T_{L,R} \delta(t - t'), \quad (3)$$

where $\langle \dots \rangle_\eta$ denotes an average over the noise.

The derivation of the linear-response theory starts with the Fokker-Planck equation for the full phase space distribution function $P(\mathbf{x}; \mathbf{v}; t)$. If $T_L = T_R = T$, the steady state solution to the equation is the equilibrium Boltzmann distribution. The perturbation approach described here can be carried through for small but arbitrary temperature variations of the baths about the equilibrium value, with the general forms $T_L(t) = T + \Delta T_L(t)$ and $T_R(t) = T + \Delta T_R(t)$. For simplicity, and for ease of comparison with the study in Ref. [13], we here consider the case where the temperatures at the two ends are oscillating in time as $T_{L,R} = T \pm \Delta T(t)/2$. We will obtain a perturbative solution about the equilibrium solution. The steps are very similar to the standard derivation of the fluctuation dissipation theorem. The Fokker-Planck equation corresponding to Eq. (2) is

$$\frac{\partial P}{\partial t} = - \sum_l \frac{\partial}{\partial x_l} (v_l P) - \sum_l \frac{\partial}{\partial v_l} (f_l P / m_l) + O_1 P + O_N P, \quad (4)$$

where $f_l = -\partial H / \partial x_l$ is the force acting on the l th particle. The operators O_1 and O_N come from the Langevin damping and noise on the terminal particles:

$$O_1 P = \frac{\gamma_L}{m_1} \frac{\partial}{\partial v_1} (v_1 P) + \frac{\gamma_L k_B T_L}{m_1^2} \frac{\partial^2}{\partial v_1^2} P, \quad (5)$$

$$O_N P = \frac{\gamma_R}{m_N} \frac{\partial}{\partial v_N} (v_N P) + \frac{\gamma_R k_B T_R}{m_N^2} \frac{\partial^2}{\partial v_N^2} P.$$

With $T_{L,R} = T \pm \Delta T(t)/2$, we can group terms according to their power of ΔT to obtain

$$\frac{\partial P}{\partial t} = \hat{L} P + \hat{L}^{\Delta T} P, \quad (6)$$

where

$$\hat{L}^{\Delta T} = \frac{k_B \Delta T}{2} \left[\frac{\gamma_L}{m_1^2} \frac{\partial^2}{\partial v_1^2} - \frac{\gamma_R}{m_N^2} \frac{\partial^2}{\partial v_N^2} \right]. \quad (7)$$

For $\Delta T = 0$, the steady state solution of the Fokker-Planck equation is the equilibrium Boltzmann distribution $P_0 = \exp[-\beta H] / Z$, where Z is the canonical partition function and $\beta = 1/(k_B T)$. For $\Delta T \neq 0$, we start with the equilibrium distribution at time $t = t_0$ and then let the system evolve under the full Fokker-Planck operator. Writing $P(\mathbf{x}, \mathbf{v}, t) = P_0 + p(\mathbf{x}, \mathbf{v}, t)$ and retaining terms to $O(\Delta T)$,

$$\frac{\partial p}{\partial t} = \hat{L} p + \hat{L}^{\Delta T} P_0. \quad (8)$$

Setting $t_0 \rightarrow -\infty$ we get the formal solution to the above equation:

$$p(\mathbf{x}; \mathbf{v}; t) = \int_{-\infty}^t e^{(t-t') \hat{L}} \Delta \beta(t') J_{\text{fp}}(\mathbf{v}) P_0(\mathbf{x}, \mathbf{v}) dt', \quad (9)$$

where $J_{\text{fp}}(\mathbf{v})$ is defined by

$$\left. \frac{\partial P}{\partial t} \right|_{P=P_0} = \hat{L}^{\Delta T} P_0 = (\Delta \beta) J_{\text{fp}} P_0 \quad (10)$$

from which

$$J_{\text{fp}} = \frac{\gamma_R}{2m_N} [m_N v_N^2 - k_B T] - \frac{\gamma_L}{2m_1} [m_1 v_1^2 - k_B T]. \quad (11)$$

The change in the expectation value of any observable $A(\mathbf{x}; \mathbf{v})$ is given by $\langle \Delta A \rangle_{\Delta T} = \langle A \rangle - \langle A \rangle_0$, where $\langle A \rangle = \int d\mathbf{x} \int d\mathbf{v} A(\mathbf{x}; \mathbf{v}) P(\mathbf{x}; \mathbf{v}, t)$ and $\langle A \rangle_0 = \int d\mathbf{x} \int d\mathbf{v} A(\mathbf{x}; \mathbf{v}) P_0(\mathbf{x}; \mathbf{v})$. This then takes the form

$$\langle \Delta A(t) \rangle_{\Delta T} = -\frac{1}{k_B T^2} \int_0^\infty \langle A(\tau) J_{\text{fp}}(0) \rangle \Delta T(t - \tau) d\tau, \quad (12)$$

where we have defined the equilibrium average $\langle A(t) J_{\text{fp}}(0) \rangle = \int d\mathbf{x} \int d\mathbf{v} A e^{\hat{L}t} J_{\text{fp}} P_0$ and we have used the time translational invariance of the equilibrium correlation function. In particular, we are interested in the energy current between two adjacent particles. The instantaneous current from the l th to the $l+1$ -th site is given by $j_{l+1,l} = \frac{1}{2}(v_l + v_{l+1}) f_{l+1,l}$, where $f_{l+1,l} = -\partial U(x_l - x_{l+1}) / \partial x_{l+1}$ is the force on the $l+1$ -th particle due to the l th particle. We get the average heat current flowing between any bond on the chain by

$$\langle j_{l+1,l}(t) \rangle_{\Delta T} = -\frac{1}{k_B T^2} \int_0^\infty \langle j_{l+1,l}(\tau) J_{\text{fp}}(0) \rangle \Delta T(t - \tau) d\tau. \quad (13)$$

For an oscillating temperature given by $\Delta T(t) = \Delta T(\omega)e^{i\omega t}$ this gives

$$\begin{aligned} \frac{\langle j_{l+1,l}(\omega) \rangle}{\Delta T(\omega)e^{i\omega t}} &= G_l(\omega)e^{-i\phi_l(\omega)} \\ &= -\frac{1}{k_B T^2} \int_0^\infty \langle j_{l+1,l}(\tau) J_{fp}(0) \rangle e^{-i\omega\tau} d\tau, \end{aligned} \quad (14)$$

where $G_l(\omega)$ is the magnitude of the response—computed numerically in Sec. III—and ϕ_l is the phase. The correlation function $\langle j_{l+1,l}(\tau) J_{fp}(0) \rangle$ on the right-hand side of this equation is for a system in equilibrium at temperature T .

A few comments are appropriate here. First, as shown in Ref. [13], for $\omega \rightarrow 0$ it is possible to manipulate the integrand on the right and make it proportional to the autocorrelation function of the heat current integrated over the entire chain, $\sum_l j_{l+1,l}(\tau)$, yielding a result resembling the standard Green-Kubo formula (but without the thermodynamic limit). This manipulation is not possible for $\omega \neq 0$. Thus the current response depends on l , the position inside the chain where the response is measured, as one would expect. Moreover, the correlation function involves J_{fp} , which is different from the heat current.

Second, although we have assumed that $\Delta T_L = -\Delta T_R$ to resemble the zero-frequency calculations of Ref. [13] where such an assumption is appropriate, at $\omega \neq 0$ there is no reason why one cannot treat ΔT_L and ΔT_R as independent variables. It is straightforward to extend the aforementioned derivation and obtain the response to ΔT_R and ΔT_L , with J_{fp} in Eq. (14) replaced by the first and second part of Eq. (11), respectively. For large N , one expects that the response to a oscillatory temperature perturbation at one end of the chain should only depend on the distance from that end and be the same as for a semi-infinite chain.

Finally, expressions similar to Eq. (13) can be obtained for any quantity that depends on the phase space variables of the system, not just $j_{l+1,l}(\tau)$. It does *not* apply to the heat current flowing into the system from the reservoirs, since they involve the Langevin noise η_L and η_R , and these have to be obtained indirectly. Thus Eq. (13) is valid for $l = 1$, and one also has

$$\langle d\epsilon_1(t)/dt \rangle_{\Delta T} = -\frac{1}{k_B T^2} \frac{d}{dt} \int_0^\infty \langle \epsilon_1(\tau) J_{fp}(0) \rangle \Delta T(t - \tau) d\tau. \quad (15)$$

Replacing the d/dt with a $-d/d\tau$ acting on ΔT and integrating by parts, adding this to Eq. (13), and using the fact that $j_{21}(t) + d\epsilon_1(t)/dt = j_{1,L}(t)$ (where $j_{1,L}$ is the heat current flowing in from the left reservoir), we have

$$\begin{aligned} \langle j_{1,L}(t) \rangle_{\Delta T} &= -\frac{1}{k_B T^2} \int_0^\infty \langle j_{1,L}(\tau) J_{fp}(0) \rangle \Delta T(t - \tau) d\tau \\ &\quad - \frac{1}{k_B T^2} \Delta T(t) \langle \epsilon_1(0) J_{fp}(0) \rangle. \end{aligned} \quad (16)$$

Fourier transforming, for $\Delta T(t) = \Delta T(\omega)e^{i\omega t}$, the heat current flowing from the left reservoir is

$$\left\langle \frac{j_{1,L}(\omega)}{\Delta T(\omega)} \right\rangle = -\frac{1}{k_B T^2} \int_0^\infty \langle j_{1,L}(\tau) J_{fp}(0) \rangle e^{-i\omega\tau} d\tau + \frac{\gamma_L}{m_1} k_B. \quad (17)$$

This response function has a nonzero $\omega \rightarrow \infty$ limit from the second term on the right-hand side. This is reasonable: if ΔT oscillates at a very high frequency, the effect on (\mathbf{x}, \mathbf{v}) should be negligible, but the current flowing from the left reservoir should oscillate because $\langle \eta_L(t) v_1(t) \rangle_\eta = \gamma_L k_B T_L(t) / m_1$ is proportional to the instantaneous temperature of the reservoir. The instantaneous response of Eq. (17) is a peculiarity of white noise stochastic baths and is not seen for Nose-Hoover baths, where even the heat current at the boundary is in terms of the extended phase space variables, or for a fluid system with Maxwell boundary conditions, where continuity requires that the heat current at the boundary and just inside the system should be the same. Therefore, hereafter we work with j_{21} and $j_{N,N-1}$ when we want the current at the boundaries.

Although the derivation given previously is for a one-dimensional chain, it is straightforward to see that it is valid for any system that is connected to only two reservoirs, regardless of its dimensionality.

III. NUMERICAL RESULTS

Numerical simulations to obtain the correlation function on the right-hand side of Eq. (14) were performed on three different systems, which differ in the potential of each particle. From these correlation functions we obtained $G_l(\omega)$ using Eq. (14). The velocity-Verlet algorithm was used, with a time step $\delta t = 0.005$. We verified that doubling δt does not change our results. For the largest systems, the initial equilibration time was $t_{eq} = 64 \times 10^6$, after which the dynamical equations were evolved for a time $t = 5 \times 10^8$. All the particle masses were set to 1, $\gamma_L = \gamma_R = 1$, and the reservoirs were at temperature $T = 2.0$. Figure 1 shows $G_1(\omega)$ as a function of ω , as defined by Eq. (14), for FPU chains of different lengths. The potential used was $U(x) = x^2/2 + x^4/4$, with $V(x) = 0$. An N -independent high-frequency peak and a low-frequency peak at $\omega \sim 1/N$ are seen. Higher harmonics of the low-frequency peak can be barely discerned. As the system size is increased, the low-frequency peak broadens and decreases slightly in height, but the zero-frequency response

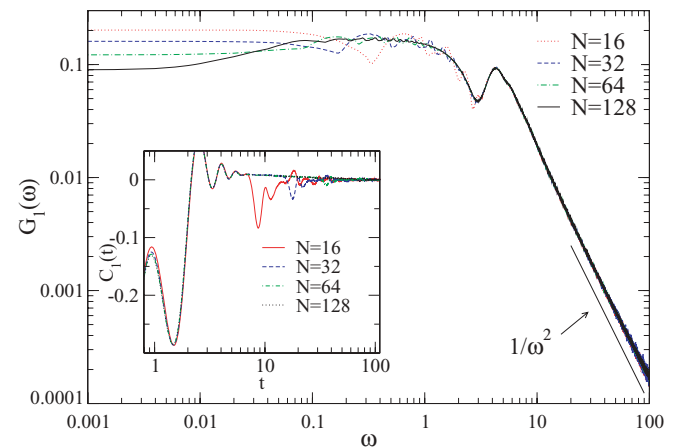


FIG. 1. (Color online) Plot of magnitude of the response function, $G_1(\omega)$, for FPU chains of different lengths. The inset shows the correlation function $C_1(t)$, which has the same information in the time domain.

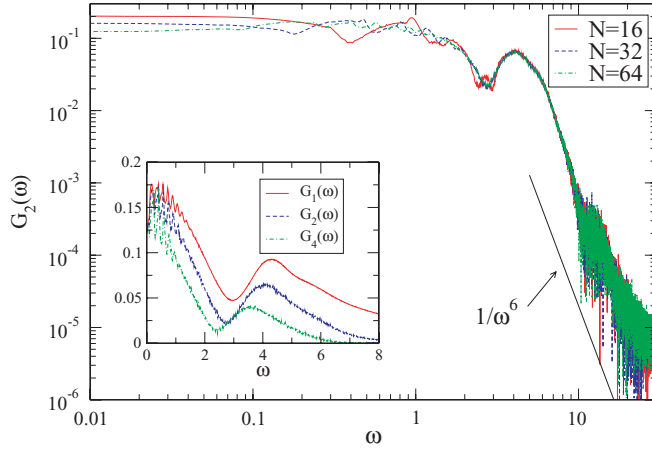


FIG. 2. (Color online) Plot of the magnitude of the response function, $G_2(\omega)$, for FPU chains of different lengths. The inset shows $G_l(\omega)$ for various $N = 64$ and various l .

drops much faster. Thus by $N = 128$, the $\omega \sim 1/N$ resonance is clearly *stronger* than the zero-frequency response. Note that Eq. (14) gives the conductance, not the conductivity; the $\omega = 0$ conductance decreases as $\sim 1/N^{1-\alpha}$. It is expected that $\alpha = 1/3$ [3] for large N but this would require much larger system sizes to verify. The inset in Fig. 1 shows $C_1(t) = \langle j_{21}(t) J_{\text{fp}}(0) \rangle$, that is, the same information in the time domain. N -independent short time oscillations that decay to (approximately) zero are seen. An “echo” of the oscillation is seen at a time τ_N that is approximately N/v , where v is possibly related to the velocity of effective phonons [16]. At high frequencies, $G_1(\omega)$ is approximately independent of N as one would expect, with a high-frequency peak. As $\omega \rightarrow \infty$, $G_1(\omega) \sim 1/\omega^2$.

Figure 2 shows $G_2(\omega)$, the magnitude of the response function at a distance $l = 2$ from the left boundary. The low-frequency peak (and its harmonics) is still present, but much more irregular in shape. However, from a device perspective, it is the currents flowing into the boundaries that are important. The high-frequency behavior is independent of N , and as seen in the inset, the peak in $G_l(\omega)$ shifts to smaller ω as l is increased. It is not clear if $G_2(\omega \sim \infty) \sim 1/\omega^6$ as is seen for the harmonic chain (discussed later in this paper).

Figure 3 shows $G_1(\omega)$ for chains of different lengths with an onsite potential $V(x) = x^4/4$. The interparticle potential is harmonic, $U(x) = x^2/2$. The dynamics are not momentum conserving, and the zero-frequency conductance should be inversely proportional to N . This is not seen in the data for two reasons: direct measurement of the zero-frequency conductance by applying a small temperature difference between the reservoirs shows that one needs $N \gtrsim 256$ to see the $\sim 1/N$ dependence, and the curves for the two larger systems (more noticeably $N = 128$) have not reached their $\omega \rightarrow 0$ limit in the figure. The low-frequency resonance is gone, replaced by a broad N -independent plateau. This is presumably because at finite temperature the effective phonons are optical instead of acoustic. The N -independent high-frequency peak is also present. The response in the interior of the chain, shown in Fig. 4 is similar, except that the low-frequency plateau extends down to $\omega = 0$ (or to very small ω). As for the FPU chains, we

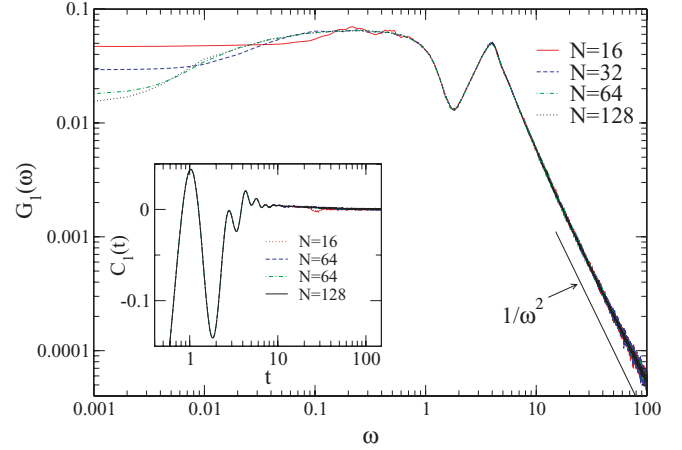


FIG. 3. (Color online) Plot of the magnitude of the response function, $G_1(\omega)$, for ϕ^4 chains of different lengths. The inset shows $C_1(t)$.

fit $G_1(\omega \sim \infty)$ to $\sim 1/\omega^2$ and—less successfully— $G_2(\omega \rightarrow \infty)$ to $\sim 1/\omega^6$. From the inset in Fig. 4, there is no significant l dependence to the location of the high-frequency peak in $G_l(\omega)$, unlike what we saw for FPU chains.

Beyond the $\sim 1/N$ dependence of the zero-frequency conductance, one expects that heat transport in systems that are not momentum conserving should be diffusive, and the temperature field will satisfy $\partial T_l / \partial t = D(T_{l+1} - 2T_l + T_{l-1})$, where $D = \kappa/C$ is the diffusion constant. With an $\sim e^{i\omega t}$ time dependence, the resultant difference equation can be solved with $T_L(\omega)$ and $T_R(\omega)$ specified, and then the heat current $j_{l+1,l} = \kappa(T_l - T_{l+1})$ can be calculated. Some features of the solution are $G_l^{\text{diff}}(\omega = 0) \propto 1/N$, $G_l^{\text{diff}}(\omega)$ is independent of N for $N \rightarrow \infty$, $G_l^{\text{diff}}(\omega \rightarrow 0) \sim \omega^{1/2} \exp[-(\omega/2D)^{1/2}l]$, and $G_l^{\text{diff}}(\omega \rightarrow \infty) \sim 1/\omega^l$. In Fig. 5 we plot the responses G_l^{diff} together with the linear-response results G_l for the ϕ^4 model. For each system size we fix the diffusion constant D so that the $\omega = 0$ results for the two responses match. One expects that the low-frequency agreement between the two sets should

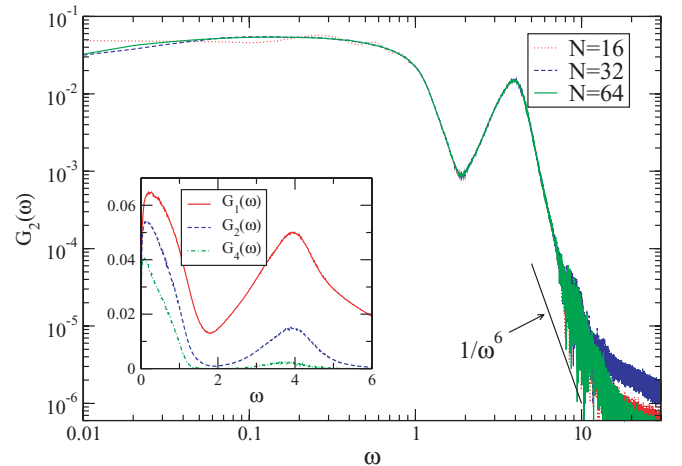


FIG. 4. (Color online) Plot of $G_2(\omega)$ for ϕ^4 chains of different lengths. A fit to $\sim 1/\omega^6$ in the asymptotic high-frequency regime is shown. The inset has $G_l(\omega)$ for various l and $N = 64$.

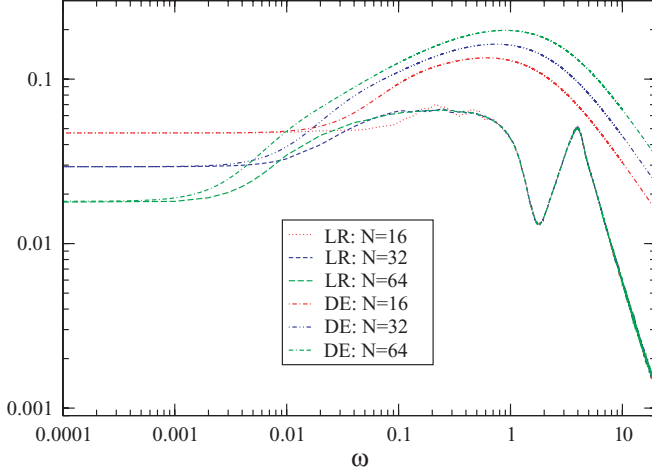


FIG. 5. (Color online) Plot of $G_1(\omega)$ for ϕ^4 chains of different lengths (LR) and $G_1^{\text{diff}}(\omega)$ from the diffusion equation (DE).

become better with increasing system size. However this is not clear from our data. At high frequencies, the expectation $G_1^{\text{diff}}(\omega) \sim 1/\omega$ is definitely not borne out. Since the diffusion equation is not expected to be valid at microscopic time or length scales, and the fact that $\sim 1/N$ scaling of the zero-frequency heat conductance is only seen for $N \gtrsim 256$ suggests that “microscopic” length scales are quite large here, the lack of agreement at the single bond level and high frequencies is perhaps not surprising. A clear understanding of this requires further work.

Finally, we show the results for a harmonic chain, with $V(x) = 0$ and $U(x) = x^2/2$. In this case we show in the next section (Sec. IV) that the response $G_l(\omega)$ can be obtained exactly and expressed in terms of a single integral over frequencies. Here we give numerical results for $G_l(\omega)$ obtained using this exact formula [Eq. (21)] and also compare it with the linear-response result [Eq. (14)]. We show $G_l(\omega)$ in Fig. 6, with results from numerical simulations of the linear-response formula also shown for $N = 64$. We see excellent agreement between the analytical and linear-response result. One can see that $G_l(\omega = 0)$ is almost N independent as expected, and the low-frequency resonance and its harmonics are more pronounced than those for the FPU chain, which is not surprising since there is no dispersion or damping in the interior of the chain. The high-frequency peak seems to be present but is difficult to cleanly separate from the low-frequency structure. As was the case for the FPU and ϕ^4 chains, $G_l(\omega \rightarrow \infty)$ is N independent and $\sim 1/\omega^2$. In Sec. IV, the asymptotic form $G_l(\omega \rightarrow \infty) \sim 1/\omega^{4l-2}$ is obtained. Figure 7 shows $G_2(\omega)$ for various system sizes, with all features as expected.

IV. RESPONSE OF A HARMONIC CHAIN

Although the integrability of the harmonic oscillator chain makes its behavior nongeneric, and its applicability to physical systems limited, the advantage of this model is that its response can be completely obtained analytically (with some integrals evaluated numerically) and compared to the simulation results. We now proceed with the analysis.

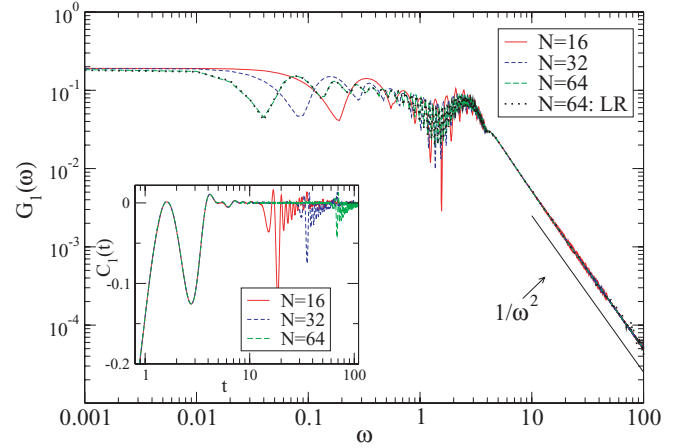


FIG. 6. (Color online) Plot of $G_1(\omega)$ for harmonic chains of different lengths, from the analytical expression derived in Sec. IV. Because of the complicated structure in the figure, $N = 128$ is not included. The linear-response simulation results for $N = 64$ are also shown (LR). The inset shows $C_1(t)$.

In this case both $V(x)$ and $U(x)$ are quadratic and the Hamiltonian can be written in the form $H = \dot{X}M\dot{X}/2 + X\Phi X/2$, where M and Φ are, respectively, the mass matrix and the force-constant matrix for the system. We obtain the solution of the equations of motion in the time-dependent steady state by using Fourier transforms in the time domain. The approach is similar to that used in the derivation of the Landauer-type formula for steady state heat current in harmonic systems, where the current is expressed in terms of phonon Green’s functions [17]. Let us introduce the transforms: $\tilde{x}_l(\Omega) = (1/2\pi) \int_{-\infty}^{\infty} dt x_l(t) e^{i\Omega t}$ and $\tilde{\eta}_{L,R}(\Omega) = (1/2\pi) \int_{-\infty}^{\infty} dt \eta_{L,R}(t) e^{i\Omega t}$. Then the Fourier transform solution of Eq. (2) gives

$$\tilde{x}_l(\Omega) = \mathcal{G}_{l1}^+(\Omega) \tilde{\eta}_L(\Omega) + \mathcal{G}_{lN}^+(\Omega) \tilde{\eta}_R(\Omega), \quad (18)$$

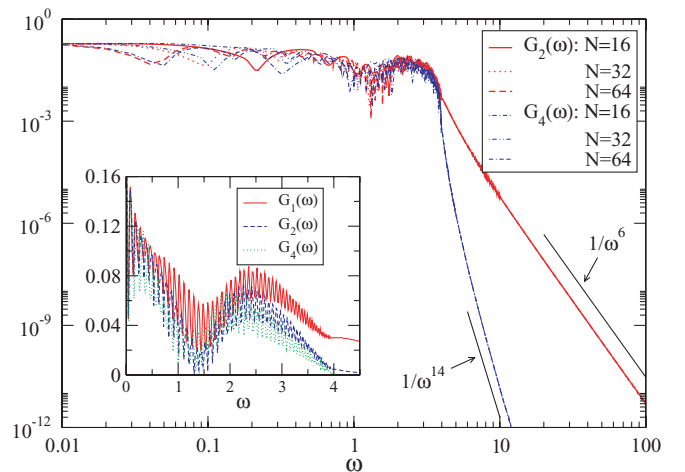


FIG. 7. (Color online) Plot of $G_2(\omega)$ and $G_4(\omega)$ for harmonic chains of various lengths. The fit to the asymptotic form $G_l(\omega \rightarrow \infty) \sim 1/\omega^{4l-2}$ is shown. The inset shows $G_l(\omega)$ for various l and $N = 64$.

where $\mathcal{G}^+(\Omega) = [-M\Omega^2 + \Phi - \Sigma^+(\Omega)]^{-1}$ is the phonon Green's function [17] and Σ^+ , the self-energy correction due to baths, is a $N \times N$ matrix whose only nonzero elements are $\Sigma_{11}^+ = i\Omega\gamma_L$ and $\Sigma_{NN}^+ = i\Omega\gamma_R$. The noise correlations corresponding to the oscillating temperatures $T_L = T + \Delta T/2 \cos \omega t$ and $T_R = T - \Delta T/2 \cos \omega t$ are given by

$$\begin{aligned} \langle \tilde{\eta}_L(\Omega_1) \tilde{\eta}_L(\Omega_2) \rangle &= \frac{\gamma_L k_B}{\pi} \{ T \delta(\Omega_1 + \Omega_2) \\ &\quad + (\Delta T/4) [\delta(\Omega_1 + \Omega_2 + \omega) \\ &\quad + \delta(\Omega_1 + \Omega_2 - \omega)] \}, \\ \langle \tilde{\eta}_R(\Omega_1) \tilde{\eta}_R(\Omega_2) \rangle &= \frac{\gamma_R k_B}{\pi} \{ T \delta(\Omega_1 + \Omega_2) \\ &\quad - (\Delta T/4) [\delta(\Omega_1 + \Omega_2 + \omega) \\ &\quad + \delta(\Omega_1 + \Omega_2 - \omega)] \}, \end{aligned} \quad (19)$$

and $\tilde{\eta}_L$ and $\tilde{\eta}_R$ are uncorrelated. The heat current on any bond is given by the noise average $\langle j_{l+1,l} \rangle = \langle (1/2)(k(x_l - x_{l+1})(v_l + v_{l+1})) \rangle$, where k is the force constant of the bonds, and thus involves evaluating

$$\begin{aligned} \langle x_l(t) v_m(t) \rangle &= \int_{-\infty}^{\infty} d\Omega_1 \int_{-\infty}^{\infty} d\Omega_2 (-i\Omega_2) e^{-i(\Omega_1 + \Omega_2)t} \\ &\quad \times [\mathcal{G}_{l1}^+(\Omega_1) \mathcal{G}_{m1}^+(\Omega_2) \langle \tilde{\eta}_L(\Omega_1) \tilde{\eta}_L(\Omega_2) \rangle \\ &\quad + \mathcal{G}_{lN}^+(\Omega_1) \mathcal{G}_{mN}^+(\Omega_2) \langle \tilde{\eta}_R(\Omega_1) \tilde{\eta}_R(\Omega_2) \rangle], \end{aligned} \quad (20)$$

and this is readily evaluated using the noise properties in Eq. (19). After some simplifications we finally obtain

$$\begin{aligned} G_l(\omega) &= \left| \frac{1}{4\pi} \int_{-\infty}^{\infty} d\Omega \Omega [\gamma_L \{ \mathcal{G}_{l1}^+(\Omega - \omega) - \mathcal{G}_{l+1,1}^+(\Omega - \omega) \} \right. \\ &\quad \times \{ \mathcal{G}_{l1}^+(-\Omega) + \mathcal{G}_{l+1,1}^+(-\Omega) \} \\ &\quad - \gamma_R \{ \mathcal{G}_{lN}^+(\Omega - \omega) - \mathcal{G}_{l+1,N}^+(\Omega - \omega) \} \\ &\quad \left. \times \{ \mathcal{G}_{lN}^+(-\Omega) + \mathcal{G}_{l+1,N}^+(-\Omega) \} \right|. \end{aligned} \quad (21)$$

For nearest-neighbor interactions, the force matrix Φ is a tridiagonal matrix. Using the properties of inverse of a tridiagonal matrix we can explicitly evaluate the Green's function elements that are required. For simplicity consider the case $k = 1$, no external potentials and $\gamma_L = \gamma_R = \gamma$. Let us define $\Delta_{l,m}$ as the determinant of the submatrix of $[-M\Omega^2 + \Phi - \Sigma^+]$ that starts from the l th row and column and ends in the m th row and column. We also define $D_{l,m}$ as the determinant of the submatrix of $[-M\Omega^2 + \Phi]$ starting from the l th row and column and ending in the m th row and column. In terms of these one has

$$\mathcal{G}_{l,1}^+(\Omega) = \frac{\Delta_{l+1,N}}{\Delta_{1,N}}, \quad \mathcal{G}_{l,N}^+(\Omega) = \frac{\Delta_{1,l-1}}{\Delta_{1,N}},$$

with

$$\begin{aligned} \Delta_{l,l-1} &= D_{l,l-1} - i\Omega\gamma D_{2,l-1}, \\ \Delta_{l+1,N} &= D_{l+1,N} - i\Omega\gamma D_{l+1,N-1}, \\ \Delta_{1,N} &= D_{1,N} - i\Omega\gamma(D_{1,N-1} + D_{2,N}) - \Omega^2\gamma^2 D_{2,N-1}. \end{aligned}$$

For an ordered harmonic chain with all masses equal to 1 it is easy to show that $D_{l,m} = \sin(m-l+2)q/\sin q$, where

$\Omega^2 = 2(1 - \cos q)$. Using this it is easy to numerically evaluate the response function $G_l(\omega)$ in Eq. (21) for given values of l and N . We show some numerical results in Figs. 6 and 7, where we have also made comparisons with results from simulations for the linear response. As expected the exact response and the linear response give almost identical results. However we have not been able to analytically show the equivalence of the exact-response and the linear-response expressions.

For large Ω , we have $q \sim \pi + i \ln \Omega^2$; hence

$$\mathcal{G}_{l,1}^+(\Omega) \sim 1/(-\Omega^2)^l. \quad (22)$$

This can also be seen from the equations of motion: when $\Omega \gg 0$, the dynamical equations become $-m_l \Omega^2 x_l = k x_{l-1}$. The boundary condition is $-m_1 \Omega^2 x_1 = \eta_L(\Omega)$, in which the right-hand sign is effectively unity when calculating the Green's function. Combining these equations, we obtain Eq. (22). But a $\sim 1/(-\Omega^2)^l$ dependence at large frequencies implies that the $2l$ th derivative of $\mathcal{G}_{l,1}^+(t)$ has a δ function at the origin; that is, $\mathcal{G}_{l,1}^+(t) \sim t^{2l-1}$ for $t \gtrsim 0$ (This can be verified directly in the time domain: $x_l(t) \propto t^{2l-1}$ satisfies the equations of motion for $t \gtrsim 0$.) But then in the time domain, Eq. (21) is equivalent to $G_l(t) \propto \mathcal{G}_{l,1}^+(t) \partial_t \mathcal{G}_{l,1}^+(t)$ for $t \gtrsim 0$, where we have assumed that l is in the left half of the chain. Therefore $G_l(t \gtrsim 0) \propto t^{4l-3}$. Since $G_l(t < 0) = 0$, the $4l - 2$ -th derivative of $G_l(t)$ has a δ function at $t = 0$, so that

$$G_l(\omega) \sim 1/\omega^{4l-2}, \quad l < N/2, \quad (23)$$

for large ω .

V. DISCUSSION

In this paper, we have given an exact linear-response formula for the current in a wire in response to time-dependent temperatures applied at the boundaries. For a harmonic chain the full response function has been analytically computed. We have presented numerical results for the frequency dependence of the current response in oscillator chains. For a diffusive system we find that the response differs from what is expected from a solution of the Fourier equation with oscillating boundary temperatures. It is straightforward to generalize the derivation to fluid systems, various stochastic and deterministic baths, and arbitrary system size L and spatial dimension d . This is discussed in detail in Ref. [13] for the $\omega = 0$ case.

As shown in Ref. [13] the zero-frequency response can be expressed in terms of current autocorrelation functions, $C_{JJ}(t) = \langle J(t)J(0) \rangle$, as opposed to the correlations involving J_{fp} in Eq. (14), resulting in an expression similar to the standard Green-Kubo formula but without the thermodynamic limit being taken. If the integral of the autocorrelation function remains finite in the thermodynamic limit, the conductance is $\sim 1/N$ for large N , and one can define an N -independent conductivity in the same regime. The resultant expression matches the standard Green-Kubo formula, but with the thermodynamic limit taken *after* the range of the integral is

taken to infinity. While it is plausible to assume that the order of limits commutes and

$$\lim_{L \rightarrow \infty} \frac{1}{L} \lim_{t_0 \rightarrow \infty} \int_0^{t_0} C_{JJ}(t) dt = \lim_{t_0 \rightarrow \infty} \lim_{L \rightarrow \infty} \frac{1}{L} \int_0^{t_0} C_{JJ}(t) dt, \quad (24)$$

this is by no means trivial: if different boundary conditions had been employed, with hard wall boundaries instead of heat baths, the left-hand side of this equation would be zero but the right-hand side would not. If the left-hand side (with heat bath boundary conditions) diverges in the thermodynamic limit, as for integrable systems or low-dimensional momentum

conserving systems, the conductivity also diverges, and one can only talk about the conductance or an L -dependent conductivity.

At nonzero frequencies, the integral converges even when it does not at $\omega = 0$, and changing the order of limits is more benign. Unfortunately, as we have seen in this paper, the expression obtained for the finite-frequency conductance involves the correlation function $\langle j_{l+1,l}(\tau) J_{\text{fp}}(0) \rangle$, which we are unable to convert into an autocorrelation function when $\omega \neq 0$. The connection to proposed expressions for the finite-frequency conductivity [9,10], which involve expressions in terms of $C_{JJ}(t)$, is thus not clear.

-
- [1] F. Bonetto, J. L. Lebowitz, and L. Rey-Bellet, in *Mathematical Physics 2000*, edited by A. Folka, A. Grigoryan, T. Kibble, and B. Zegarlinski (Imperial College Press, London, 2000).
- [2] S. Lepri, R. Livi, and A. Politi, *Phys. Rep.* **377**, 1 (2003).
- [3] A. Dhar, *Adv. Phys.* **57**, 457 (2008).
- [4] E. Fermi, J. Pasta, and S. Ulam, *Studies of Nonlinear Problems*, Los Alamos Document LA-1940, 1955.
- [5] C. W. Chang, D. Okawa, H. Garcia, A. Majumdar, and A. Zettl, *Phys. Rev. Lett.* **101**, 075903 (2008); D. Li, Y. Wu, P. Kim, L. Shi, P. Yang, and A. Majumdar, *Appl. Phys. Lett.* **83**, 2934 (2003).
- [6] P. K. Dixon and S. R. Nagel, *Phys. Rev. Lett.* **61**, 341 (1988).
- [7] J. S. Olafsen and R. P. Behringer, *J. Low Temp. Phys.* **117**, 53 (1999).
- [8] N. O. Birge, *Phys. Rev. B* **34**, 1631 (1986).
- [9] B. S. Shastry, *Phys. Rev. B* **73**, 085117 (2006).
- [10] S. G. Volz, *Phys. Rev. Lett.* **87**, 074301 (2001).
- [11] N. Li, P. Hanggi, and B. Li, *Europhys. Lett.* **84**, 40009 (2008).
- [12] J. Ren and B. Li, *Phys. Rev. E* **81**, 021111 (2010).
- [13] A. Kundu, A. Dhar, and O. Narayan, *J. Stat. Mech.* (2009) L03001.
- [14] M. S. Green, *J. Chem. Phys.* **22**, 398 (1954); R. Kubo, M. Yokota, and S. Nakajima, *J. Phys. Soc. Jpn.* **12**, 1203 (1957).
- [15] J. M. Deutsch and O. Narayan, *Phys. Rev. E* **68**, 041203 (2003).
- [16] N. Li, B. Li, and S. Flach, *Phys. Rev. Lett.* **105**, 054102 (2010).
- [17] A. Dhar and D. Roy, *J. Stat. Phys.* **125**, 801 (2006).